velocity at sea level of these units represents a viable solution to the problem of ground impact damage that has plagued almost all space nuclear heat source programs to date.

References

[1] Brunner, M. J., Dohner, C. V., and Lawit, R. L., "Re-Entry of Radioactive Power Sources," *Journal of Spacecraft and Rockets*, Vol. 5, No. 4, April 1968, pp. 448–453.

[2] Bustamante, A. C. and Stone, G. W., Jr., "The Dynamic Characteristics of Autorotating Configurations in Subsonic and Hypersonic Flows," SC-DE-682395, Nov. 1968, Sandia Labs., Albuquerque, N.Mex.

[3] Dix, G. P., "Advances in the Safety of Space Nuclear Power Systems," Second International Symposium on Power from Radioisotopes, European Nuclear Energy Agency and Spanish Junta on Atomic Energy, Madrid, Spain, May 1972.

[4] La Porte, A. H. and Osmeyer, W. E., "Growth Potential of the Snap 19 High Performance Generator Through Technology Application," International Conference on Nuclear Solutions to World Energy Problems, American Nuclear Society, Washington, D.C., Nov. 1972.

[5] Vorreiter, J. W. and Tate, D. L., "Observations of Disk-Shaped Bodies in Free Flight at Terminal Velocity," TM X-62, 262, 1973, NASA.

[6] Hogfors, H. E., "Velocity-Flight Path Envelopes for Different Failure Modes in a Titan IIIC Synchronous Mission," TOR-0172-(2701-01)-5, March 6, 1973, Aerospace Corp., El Segundo, Calif.

[7] Bustamante, A. C., Randall, D. E., and McAlees, S., "Have Sinew-1 Postflight Report," SC-RR-72 0225, May 1972, Sandia Labs., Albuquerque, N.Mex.

[8] Marvin, J. G. and Sinclair, A. R., "Convective Heating in Regions of Large Favorable Pressure Gradient," *AIAA Journal*, Vol. 5, No. 11, Nov. 1967, pp. 1940–1948.

[9] Kreith, F., *Principles of Heat Transfer*, International Textbook Co., Scranton, Pa., 1958, p. 379.

[10] Inouye, M., Marvin, J. G., and Sinclair, A. R., "Comparison of Experimental and Theoretical Shock Shapes and Pressures Distributions on Flat-Faced Cylinders at Mach 10.5," TN D-4397, 1968, NASA.

[11] "Mechanical and Thermal Properties of MOD-3 Billets 727 and 731," Purchase Order 236041, Prime Contract F33615-70-C-1587, April 28, 1972, Southern Research Inst., Birmingham, Ala.

[12] Metzger, J. W., Engel, M. J., and Diaconis, N. S., "The Oxidation and Sublimation of Graphite in Simulated Re-Entry Environments," AIAA Paper 65-643, Monterey, Calif., 1965.

[13] Scala, S. M. and Gilbert, L. M., "Aerothermochemical Behavior of Graphite at Elevated Temperatures," Rept. R63SD89, Nov. 1963, General Electric, King of Prussia, Pa.

[14] Scala, S. M. and Gilbert, L. M., "Sublimation of Graphite at Hypersonic Speeds," *AIAA Journal*, Vol. 3, No. 9, Sept. 1965, pp. 1635–1644.

MAY 1974 J. SPACECRAFT VOL. 11, NO. 5

Four Space Shuttle Wing Leading Edge Concepts

G. A. NIBLOCK* AND J. C. REEDER†
McDonnell Douglas Astronautics Company-East, St. Louis, Mo.

AND

F. HUNEIDI‡
Marshall Space Flight Center, Huntsville, Ala.

A heat-pipe-cooled Space Shuttle orbiter wing leading edge was compared and evaluated against three alternate leading edge candidates: a refurbishable ablative design, and two other reusable versions employing coated columbium and carbon-carbon high-temperature segments. Each candidate concept was shown feasible in the Phase B environment. The reusable versions were all found to cost nearly the same and substantially less than the nonreusable ablative version.

Nomenclature

Aw = cross sectional area of wick
g = acceleration
g_c = gravitational constant
h_{fg} = heat of vaporization
K_p = permeability constant
$K_p A_w/W$ = wick design parameter
q_o = stagnation heat flux
$q(x)$ = local heat flux
$q(x)/q_o$ = ratio of local to stagnation heat flux
r_c = capillary radius
W = wick thickness
x = distance along heat pipe axis
Z = axial length
ΔP_c = available capillary pumping pressure rise
ΔP_g = pressure due to gravity
ΔP_L = liquid pressure drop
ΔP_v = vapor pressure drop
θ = contact angle
μ_L = liquid viscosity
μ_v = vapor viscosity
ρ_L = liquid density
σ = surface tension
ϕ = angle between axis of heat pipe and acceleration vector

Presented as Paper 73-738 at the AIAA 8th Thermophysics Conference, Palm Springs, Calif., July 16–18, 1973; submitted August 15, 1973; revision received November 30, 1973.

Index categories: Spacecraft Temperature Control Systems; Structural Design, Optimal.

* Senior Thermodynamics Engineer.

† Senior Strength Engineer.

‡ Technical Assistant to Thermal Engineering Branch Chief, Astronautics Laboratory.

I. Introduction

THE goal of low-cost space transportation that the Space Shuttle is expected to accomplish requires reusable system components. The orbiter will make about 100 flights in fulfilling its design capability. During the flights the nose region and leading edge surfaces experience an extremely severe environment.

A study was performed under Contract NAS 8-27708 to examine the feasibility of using high-temperature heat pipes for cooling nose and wing stagnation regions and three alternate concepts for the wing application. The orbiter leading edge heat

pipe application was found to be feasible with respect to the heating and acceleration environments.

A Space Shuttle orbiter leading edge heat pipe design and three alternates were examined and are presented in this paper. Alternate TPS designs (ablative, carbon-carbon, and columbium) were explored for comparison with the heat pipe leading edge. The heat pipe version was determined to be somewhat heavier than then alternate candidates but much less expensive than the ablative version (as was each reusable design) on the basis of total program costs.

II. Leading Edge Cooling

Leading Edge Cooling with Heat Pipes

The intent of leading edge cooling with heat pipes is to permit the use of less expensive materials for construction of a fully reusable structure. The heat pipes are formed to match the shape of the leading edge and are installed in a roughly chordwise orientation. Heat pipes provide cooling by transferring heat from the stagnation region to cooler regions aft of the stagnation line. High heating near the stagnation line vaporizes the working fluid. The vapor then flows axially through the pipe to the aft portion, which experiences lower heating. Because this section is cooler, the vapor condenses, rejecting the heat absorbed near the stagnation line. The condensed liquid is returned in an internal wick to the evaporating region by capillary action. The effect produced is a reduction of the stagnation region temperature, accompanied by a temperature increase in the aft portion of the leading edge. The high heat transfer accomplished by heat pipes in effect averages the temperature along the axis of the pipe.

The reduction in stagnation temperature using heat pipes can be substantial. The design goal in the contracted study was a reduction from 1330°C (2400°F) to 1000°C (1800°F) to allow substitution of a superalloy for columbium. Study results indicate such a reduction is feasible with sodium heat pipes. It should be noted, however, that the magnitude of the temperature reduction is strongly dependent on the heating distribution and the configuration of the leading edge.

Design of an optimized heat-pipe-cooled leading edge must consider each stage of the operational cycle. For example, vapor pressure of the sodium varies from near zero at low temperatures to about 4.14 (10^5) N/m^2 (60 lb/in.^{2}) when the heat pipes are operating at capacity. Heat pipes thus are vacuum bottles on the ground, but pressure vessels during entry. To be structurally efficient, the heat pipes must be an integral part of leading edge structure. The working fluid must be chemically compatible with the wick and container at high temperatures. Finally, heat pipe thermal performance analysis is required to assure that the pipes have the required heat transfer capacity and startup characteristics.

Working Fluid Selection

Selection of working fluid is heavily dependent on the temperature range of interest. Two temperature levels were considered: 1000°C (1830°F); and 1300°C (2370°F), which correspond to maximum reuse levels for superalloys and refractory metals, respectively.

Selection of working fluid involves: 1) an evaluation of thermophysical properties of candidate fluids and their relationship with operational limits of the system; 2) compatibility considerations; 3) effect of fluid on design of other system elements, such as the wick and container; and 4) over-all system considerations, such as weight, safety, startup, etc.

In liquid metal systems using high-thermal-conductivity fluids, boiling has seldom been a limiting condition and the peak design heat flux of 295 kw/m^2 (26 Btu/ft^2-sec) was well below maximum obtainable values. Entrainment was not a limiting condition for this system if an isotropic wick was used to accommodate the acceleration forces. Performance of working fluids, therefore, was based on pumping and sonic limit considerations. Absolute pumping limit performance cannot be calculated without specifying the other elements of the system; namely, the wick and container design. Relative performance, however, is measured in terms of 0-g and 1-g figure of merit (FOM) curves. The 0-g FOM curve relates maximum performance when frictional losses dominate. If vapor losses and gravity effects are neglected, the pressure balance can be expressed as follows:

$$\Delta P_L = \Delta P_C \quad \text{which yields after substitution}$$

$$\frac{\mu_L Z q_o \int\int [q(x)/q_o]\, dx\, dx}{K_p A_w \rho_L h_{f_g}} = \frac{2\sigma \cos\theta}{r_c}$$

Since the contact angle (θ) is small with a liquid which wets the surface, a necessity for heat pipe operation, the preceding relation may be rearranged as

$$q_o \int\int \frac{q(x)}{q_o}\, dx\, dx = \left(\frac{\sigma \rho_L h_{f_g}}{\mu_L}\right)\left[\frac{2K_P A_w}{r_c Z}\right]$$

The term in parentheses contains only physical properties of the working fluid and the term in brackets contains terms relating only to geometry of the heat pipe. Thus, for a given heat pipe design, the term in brackets is a constant and only the physical properties of the working fluid are variables. The term in parentheses is commonly called the FOM for 0-g, thus

$$(\text{FOM})_{og} = \sigma \rho_L h_{fg}/\mu_L$$

From the preceding equation it can be seen that the highest heat transport capability will be obtained with fluid possessing the highest FOM.

If the heat pipe must operate against a gravity head such that both the liquid and vapor pressure drops are insignificant compared with the gravity head, ΔP_L and $\Delta P_v << \Delta P_g$, another FOM is appropriate. This FOM for gravity fields is developed as follows:

$$\Delta P_c = \Delta P_g$$

or

$$\frac{2\sigma \cos\theta}{r_c} = \rho_L g \cos\phi \left(\frac{g}{g_c}\right) \quad \text{after substitution}$$

From this the capillary pumping capacity given by

$$h \cos\phi = \left(\frac{\sigma}{\rho_L}\right)\left[\frac{2}{r_c}\frac{g_c}{g}\right] \quad \text{since } \cos\theta \to 1$$

with the term in parentheses defined as the 1-g FOM

$$\text{FOM}_{1g} = \sigma/\rho_L$$

Both FOM are functions of temperature since they represent the physical properties of the fluid.

On the basis of either FOM, lithium presented the best choice as a high temperature working fluid. The most appropriate liquid metal working fluid was not, however, selected solely on the basis of the FOM. Selecting the fluid with the highest FOM only guarantees that the predicted performance will be the highest using that fluid. Other factors, such as vapor pressure of the working fluid and corrosion behavior, can significantly affect the choice of fluid.

On examination of the physical property data, startup dynamics, and corrosion behavior, sodium was found to be the best choice for a working fluid at a temperature of 1000°C (1830°F) where the use of nickel-base superalloys was being considered. This choice was based principally on low corrosion rates, good FOM for gravity operation, and good startup capability. At the higher temperatures, where refractory metals such as columbium must be used, the best choice would be calcium, with this selection based mainly on low corrosion rates.

Safety

The safety of the proposed heat pipe working fluid must be assured in the ground handling, launch, and re-entry environments. Potential causes of hazardous exposure to heat pipe working fluids were examined. A heat pipe leading edge was found to present a minimal safety hazard.

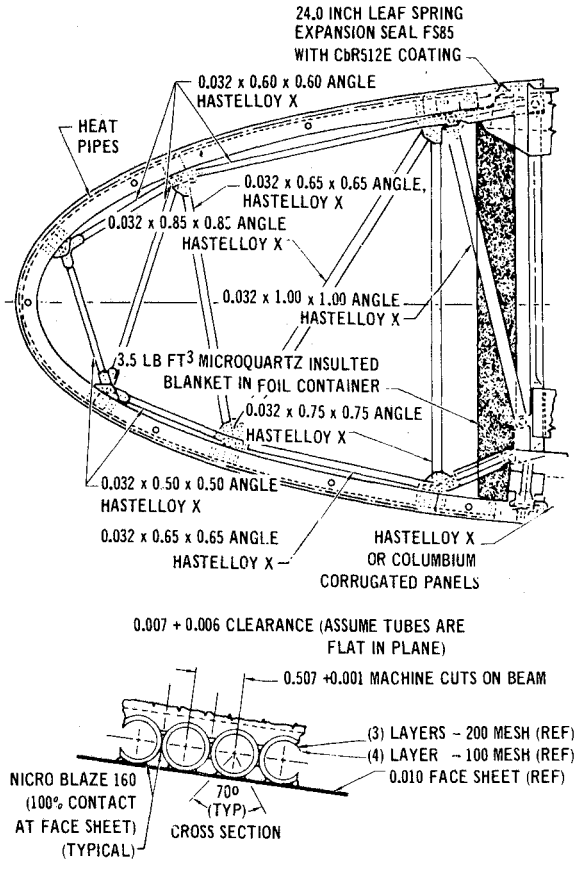

Fig. 1 Hastelloy-X heat pipe leading edge.

In the unlikely event of puncture or rupture of a sodium heat pipe, the sodium would burn in air or react with water.

Assuming a worst-case adiabatic reaction, the temperature of the mixture plus pipe section would rise rapidly to a maximum of 870°C (1565°F) over the initial temperature, well below the melting point of Hastelloy-X.

The primary hazard is essentially exposure of personnel to the working fluid. However, the working fluid is contained in a strong, tough container and should be at or near ambient temperature when the orbiter is on the ground. No transfer of hazardous fluids is required, as with hypergolic or cryogenic propellants, and the total quantity of working fluid is small. Even crash damage would be effectively localized. The details of this safety analysis have been reported in Ref. 1.

Wick Design

Four wick configurations were evaluated for this system. Closely packed composite grooves, covered grooves, and open grooves give comparable performance—all better than a homogeneous screen. Small longitudinal grooves, however, would be very difficult to fabricate in a thin-walled superalloy tube. The closely packed composite and homogeneous screen have both been used successfully, but the homogeneous screen has an advantage in simplicity of manufacture. In general, the differences in weight between the various wick concepts is not excessive. Homogeneous screen wicks were chosen because of their structural simplicity.

Wick Requirements

The general operating condition common to both the orbiter and booster, which have an effect on the wick design, are:

1) Heat pipe operation is not required during ascent, since heating rates are not high enough to cause excessive structural temperatures.

2) Heating rates during ascent, however, are high enough to melt the working fluids. Gravity forces tend to force the fluid to the condenser regions. Refilling of the evaporator region by capillary or gravity action must be ensured prior to onset of high re-entry heating rates.

3) During re-entry, the wicking structure must provide an adequate supply of working fluid to the heated regions.

Heat pipes for all systems would have a thin layer of wick on all heated surfaces to promote uniform fluid distribution and prevent thermocapillary or nucleate boiling dryout. A certain portion of the wing or leading edge must have a wicking system which can supply heat in an adverse gravity field. The surface area requiring such wicking is a function of the angle of attack. For the orbiter leading edge, analysis was performed with two fluids, calcium and sodium, corresponding to operation at 1300°C (2370°F) and 1000°C (1830°F), respectively. Angles of attack above 0.785 rad (45°), do not require wicking for pumping. For the angle of attack of 0.523 rad (30°) during high re-entry heating, 27.4 cm (10.8 in.) of wicking length are required along the windward surface.

Values of the wicking parameter $K_p A_w/W$ for calcium and sodium leading edge designs were determined as a function of angle of attack. With 200-mesh screen, the required value of $K_p A_w/W$ was less than 0.1×10^{-12} m^4/m at 0.523-rad (30°) angle of attack for either calcium or sodium. This characteristic, which is independent of the working fluid, can be used to determine wick thickness. For any selected tube size between 1.27 cm (0.5 in.) and 2.54 cm (1.0 in.), a wick thickness of 0.0381 cm (0.015 in.) is required. This amounts to a single layer even though a factor of 2 was included in the analysis to provide a margin of safety.

In addition to pumping requirements during re-entry, the wick must be designed to ensure that adequate fluid is located in the evaporator region prior to onset of high re-entry heating rates. During launch, the heating rates give temperatures sufficient to melt sodium. The high gravity forces tend to force the liquid to the aft portions of the heat pipe. Fortunately, in the case of the orbiter, the highest heating rates occur just prior to and during the coast phase of the trajectory. Ample time for redistributing sodium, which takes less than 100 sec, is available. The wick in the evaporator will be saturated prior to re-entry. These considerations, therefore, impose no additional constraint on wick design.

Heat Pipe Structural Design

Various structural configurations were evaluated based on thermal and structural requirements with weight as the principal criterion for comparison. The basic structural cross section shown in Fig. 1 consisted of a row of tubes side-by-side, brazed together, and brazed to a thin face sheet.

A cross-section optimization compared relative weights of tubular and corrugated heat pipe configurations for various

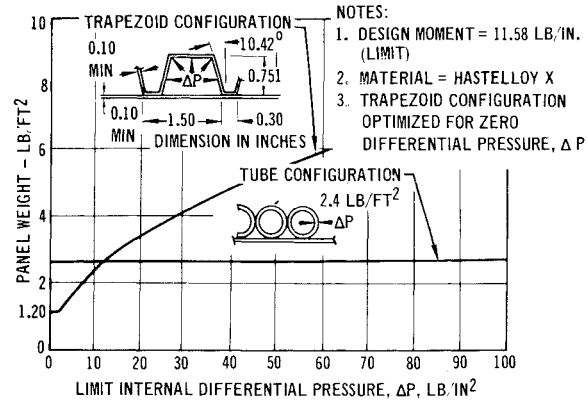

Fig. 2 Heat pipe cross section optimization.

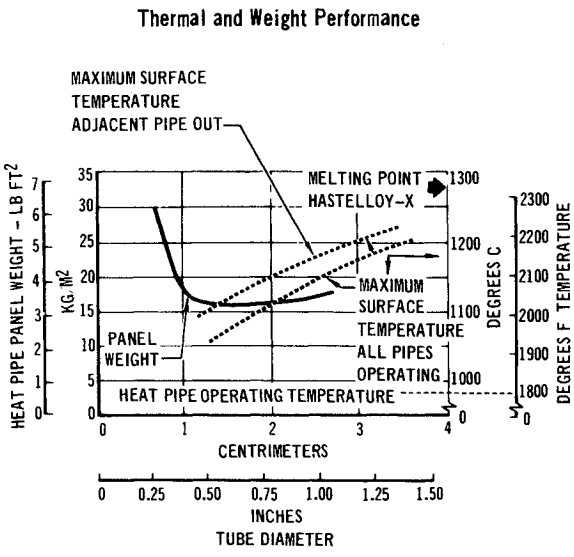

Fig. 3 Heat pipe panel.

internal vapor pressure levels, corresponding to varying temperatures. Results are shown in Fig. 2. The tubular concept was found to be lighter at all working pressure levels, because it is an efficient pressure vessel. No increase in tube wall thickness is required because of internal pressure. The corrugated configurations, having flat side walls, are inefficient pressure vessels and require relatively thick walls in order to withstand the internal pressure.

Design parameters, such as tube diameter, tube spacing, skin thickness, braze fillet size, and tube thickness, were evaluated to determine their effect on temperature gradients and weight. A steady-state heat-transfer model, specifically designed for this application, aided in this evaluation. Brazed fillet size was found to be very important, based both on weight and temperature gradient considerations. Fillets with an included angle of 70° measured from the tube center were found to be optimum in terms of weight and tube temperature gradients.

A trade study performed with the steady-state model to determine the optimum tube diameter, assuming heat pipe operation at 980°C (1800°F), is illustrated in Fig. 3. This study indicated that a tube diameter of approximately 1.9 cm (0.75 in.) results in the lightest weight system if only strength requirements are considered. Also shown in Fig. 3 is the normal maximum temperature and maximum temperature with one heat pipe non-operational, again assuming heat pipe operation at 980°C (1800°F). Maximum temperature increases with tube diameter.

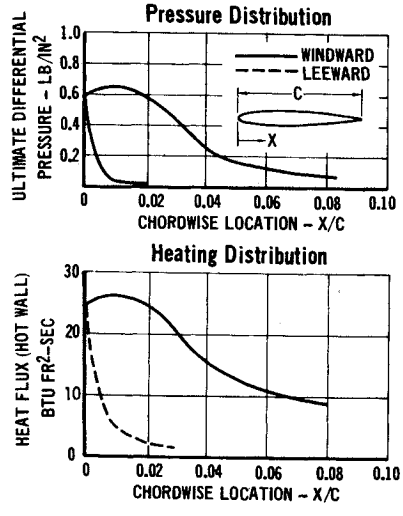

Fig. 4 Design heating and pressure distributions.

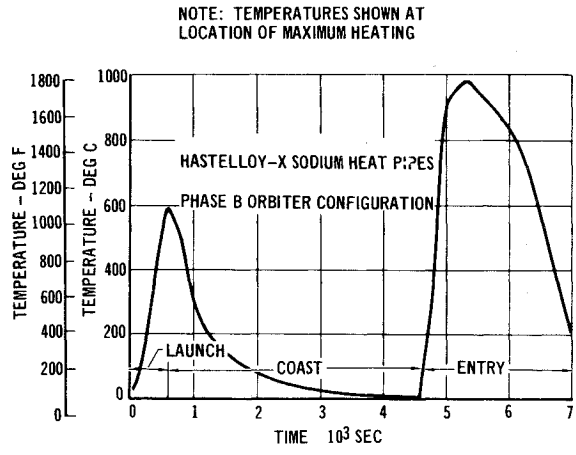

Fig. 5 Nominal heat pipe leading edge temperature.

Since the weight curve is very flat near the minimum weight, tube diameters smaller than 1.9 cm (0.73 in.) may be used while maintaining a near-minimum weight design. However, a heat pipe diameter larger than 1.27 cm (0.5 in.) permits excessive temperatures, therefore, 1.27 cm (0.50 in.) was selected.

The transient thermal performance analysis of the leading edge configuration was conducted with a three-dimensional finite-difference model. The model was comprehensive, consisting of 300 nodes and representing 2 heat pipes. The heating (and pressure) distribution is given in Fig. 4. To determine mission performance, a heating history was constructed to represent a brief but complete mission; launch, coast, and entry, assuming a single-orbit aborted flight. Results of this analysis, illustrated in Fig. 5, show the transient temperature response of the hottest spanwise location on the leading edge. The temperature history shown is for the skin at a point located on the stagnation line and midway between the heat pipes. The maximum temperature is about 980°C (1800°F), well within the capability of Hastelloy-X. This computation yielded somewhat lower heat pipe temperatures than had been assumed in the trade study. Thus, it appears larger diameter tubes might be utilized.

The over-all structural concept consisted of tubes, face sheet, and internal truss supports. All required structure was defined in detail from the forward wing edge aft to the forward spar. Truss supports were located every 50.8 cm (20 in.) along the spar. The heat pipes lay in vertical planes normal to the forward spar.

The structure was designed to withstand ultimate load at operating temperature without failure. Loads and temperatures occurring during ascent and entry determined in Phase B studies were included in the analysis. To prevent undesirable structural deformation due to creep, creep strains were limited to less than 0.5 % after 100 mission cycles. Design factor of safety on limit load for metal parts was 1.4.

A "failsafe" feature was imposed on the heat pipe design which required no structural failure at limit load if one heat pipe was inoperative. Heat pipes tubes were designed to withstand a proof pressure equal to 2.0 times operating pressure without yielding, and a burst pressure equal to 4.0 times operating pressure without failure.

A finite element model of the structure was prepared and used for analysis. The structural engineering computer program, STRUDL-II,§ was employed. External load reactions, internal loads, and displacements resulting from aerodynamic and thermal loading conditions (Fig. 4) were determined. Each truss member was designed to carry critical combinations of compressive loads and bending moments using beam-column analysis. Seven loading conditions, four occurring during ascent and three during entry, were analyzed. The truss members

§ STRUDL II is a general civil engineering computer program written by the Dept. of Civil Engineering, MIT.

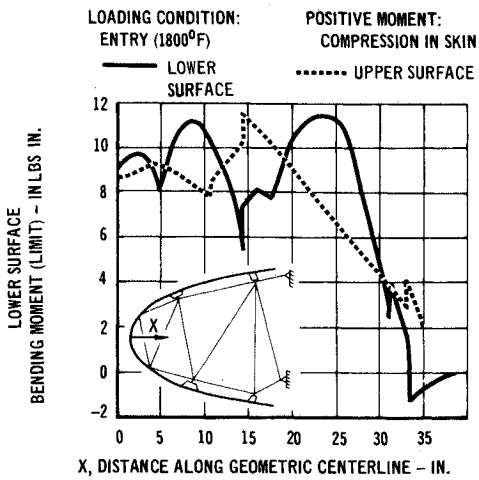

Fig. 6 Heat pipe leading edge bending moment distribution mold-line structure, Hastelloy-X material.

were found to be critical for ascent loads. For the heat pipes, the most severe condition was found to occur during entry at the time that heat pipe temperature reached a maximum. An equivalent linear temperature gradient was assumed along the length of the heat pipe. For this condition the maximum bending moments were 38.7 Nm/m (8.7 in. lb/in.) due to thermal stress and 12.8 Nm/m (2.88 in. lb/in.) due to pressure load, as shown in Fig. 6. These loads were used to size the tubes and face sheet.

III. Comparison Uncooled Leading Edges

Uncooled Leading Concepts

Three alternate leading edge TPS configurations were designed to enable a comparison with the heat-pipe-cooled design. The uncooled leading edge designs included an ablator system bonded to titanium honeycomb substructure, a carbon-carbon/Hastelloy-X structure and a columbium/Hastelloy-X structure. Each leading edge was designed for the same environment used for the heat pipe.

All leading edges were analyzed in detail in the manner described for the heat pipe leading edge using the heating and pressure distributions given previously. Generally, the ascent loading condition was most critical for the ablator, carbon-carbon, and columbium designs. The leading edge temperatures utilized in the trade study analysis are shown in Fig. 7.

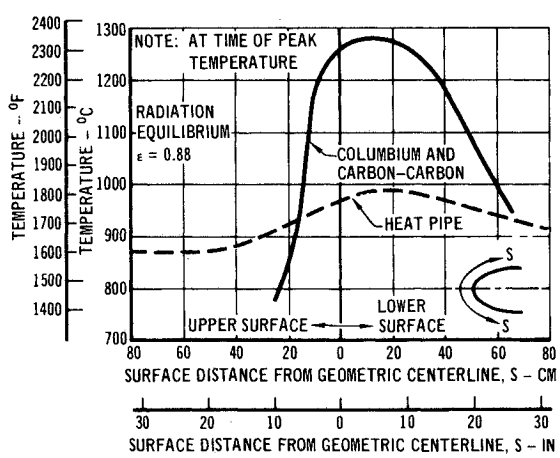

Fig. 7 Leading edge temperature distributions.

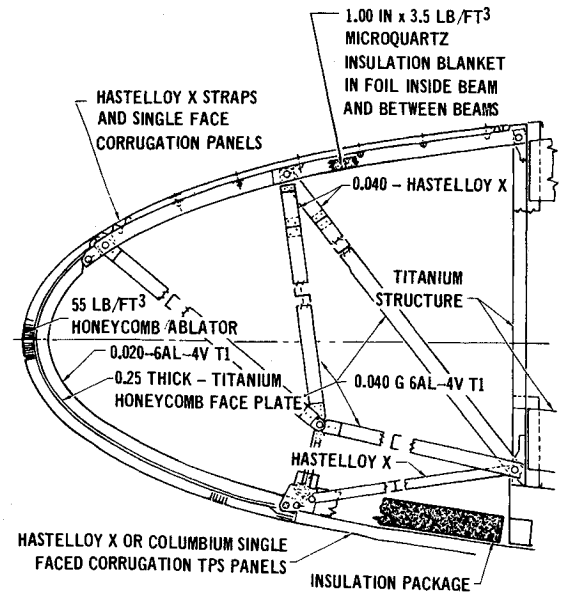

Fig. 8 Ablative leading edge.

Ablative Leading Edge

The ablative leading edge, illustrated in Fig. 8, consisted of ablative material bonded to metal substructure. A high-density (896-kg/m^3 56-lb/ft^3) MDC ablator, designated S-3, was selected to provide good resistance to aerodynamic shear. The ablator thickness was selected to give a maximum bond line temperature of 316°C (600°F). Ablator thickness requirements were calculated by the semi-empirical method of Ref. 2 from the heating distribution given in Fig. 4.

The forward section of this leading edge was a readily removable panel consisting of ablator bonded to a titanium honeycomb sandwich. The sandwich structure was 40.6 cm (16 in.) wide, framed with titanium channels and supported by a titanium truss structure. The sections were attached with quick-release fasteners. After each flight the ablative segment would be removed and taken to a refurbishment area, where the ablator would be stripped off and replaced.

Aft of the ablative section, in regions where the temperature is lower than 870°C (1600°F), the leading edge skins consisted

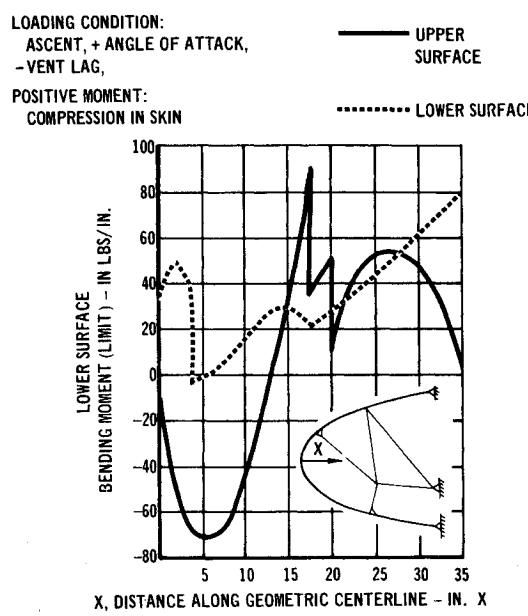

Fig. 9 Ablative or carbon-carbon leading edge bending moment distribution mold-line structure.

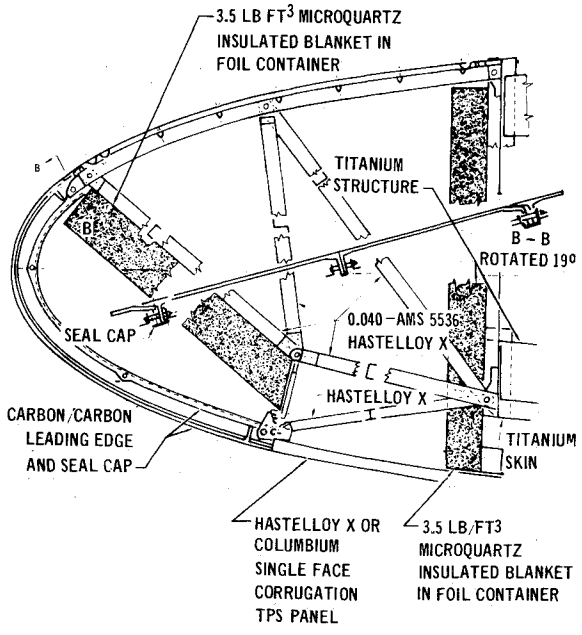

Fig. 10 Carbon-carbon leading edge.

of Hastelloy-X panels. These panels were corrugation-stiffened using a configuration developed during Phase B by MDAC-E. Optimum geometry to minimize weight of corrugated panels was determined as a function of applied pressure load using a special computer program developed for this purpose. The panels are backed with insulation blankets of 56-kg/m^3 (3.5-lb/ft^3) density insulation packaged in Inconel foil. The insulation thickness was sized to yield a backside temperature of 600°F.

The leading edge bending moment distribution for the ablative leading edge is shown in Fig. 9. Minimum practical gage honeycomb face sheet and minimum thickness core were used for the titanium panel, and analysis indicated a substantial strength margin.

Carbon-Carbon Leading Edge

The carbon-carbon leading edge is illustrated in Fig. 10. The carbon-carbon extended over the same portion of the leading edge design as the ablative and was designed for the bending moment distribution shown in Fig. 9. Aft of the carbon-carbon, Hastelloy-X single-face corrugated panels were used. The same

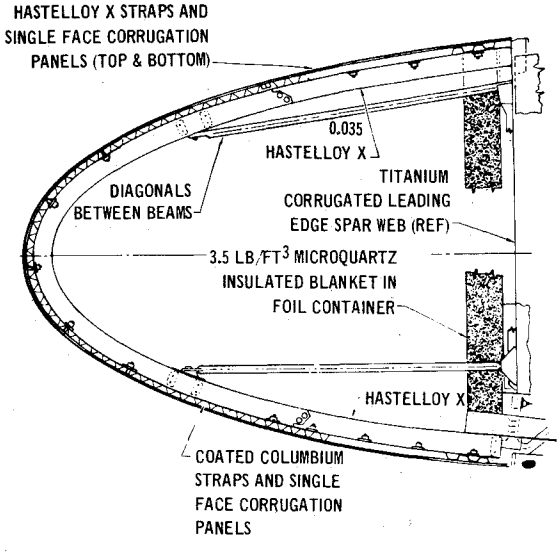

Fig. 11 Columbium leading edge.

	ABLATIVE	CARBON-CARBON	COLUMBIUM	HASTELLOY-X HEAT PIPE
RDT&E	10.40	12.61	12.19	13.87
PRODUCTION (3 VEHICLES)	3.40	4.91	4.89	5.75
*OPERATIONAL SPARES	94.16	15.77	15.74	17.32
TOTALS	107.96	33.29	32.82	36.94

*REPLACEMENT ASSUMPTIONS:
ABLATOR - 100% /FLIGHT
OTHER - 3% /FLIGHT

TOTAL PROGRAM:
5 FLIGHT VEHICLES
6 DEVELOPMENT FLIGHTS
471 OPERATIONAL FLIGHTS

Fig. 12 Leading edge concepts costs in millions of 1971 dollars total program.

type of truss work used for the ablative leading edge supported the carbon-carbon and Hastelloy-X panels. In this case the truss work was Hastelloy X instead of titanium. Stiffening ribs were provided around the perimeter of the carbon-carbon panel. Integral lugs at the four corners of the carbon-carbon assembly provide the attachment to the truss work.

The carbon-carbon element of the leading edge assembly was first modeled separately and structurally analyzed using an MDC computer program, CASD. A grid-work of beams interconnected with shear panels was used to idealize the carbon-carbon. Bending moments calculated for the beams were converted to bending moments per inch of width and used to establish the required carbon-carbon thicknesses. No allowance was made for additional thickness necessary to compensate for ablation or oxidation. Structural analysis of the complete leading edge was performed using the STRUDL II program.

Columbium Leading Edge

The columbium leading edge, Fig. 11, consisted of single-face corrugated panels supported on columbium ribs attached to the wing forward spar. The panel geometry was established to obtain a minimum weight design. Simple tubular struts supported side loads. Panel retainer straps were the same as those used on the Phase B final design. Where the maximum temperature is less than 870°C (1600°F), Hastelloy X panels are used instead of columbium panels.

IV. Comparison of Leading Edges

Leading Edge Comparative Costs

Results of the cost study for the four leading edge concepts are shown on Fig. 12. Cost estimates were based on cost estimating relationships derived from a broad mix of data sources, including Gemini, Mercury, F-4, ASSET, BGRV, S-IVB, commercial aircraft, and vendor data. The cost study assumed 5 flight vehicles, 6 development flights, and 471 operational flights. The ablator was replaced every flight. Other concepts were assumed to require 3% per flight refurbishment.

The reusable concepts cost nearly the same, with columbium being least expensive, followed closely by carbon-carbon. Uncertainties in the estimates were such that the cost differences in the reusable designs were not considered significant. The ablative leading edge, however, was substantially more expensive than the reusable concepts.

Ablative version costs are high for a multiple-use vehicle, principally because of refurbishment requirements. The largest refurbishment costs are for removal and replacement of parts, while the smallest portion of refurbishment costs are attributable to raw materials.

Leading Edge Weights

Detailed calculations of the weight of each leading edge design were prepared and results are shown in Fig. 13. The heat pipe concept was somewhat heavier than the others. The basic assumption, which led to the choice of heat pipes as a leading

HEAT PIPES			ABLATIVE	
COMPONENT	HASTELLOY-X LB/FT^2	TD-Ni-CR LB/FT^2	COMPONENT	LB/FT^2
FACESHEETS & TUBING	2.40	1.82	ABLATOR	1.95
BRAZE FILLETS	0.59	0.60	HONEYCOMB	0.42
WICK	0.38	0.40	HASTELLOY-X PANELS	0.43
WORKING FLUID	0.07	0.10	SUPPORT STRUCTURE	0.33
SUPPORT STRUCTURE	0.80	0.80	INSULATION	0.44
INSULATION	0.50	0.50		3.57
	4.94	4.22		

CARBON/CARBON		COLUMBIUM	
COMPONENT	LB/FT^2	COMPONENT	LB/FT^2
CARBON/CARBON	1.30	COLUMBIUM PANELS	0.77
HASTELLOY-X PANELS	0.53	HASTELLOY-X PANELS	0.60
SUPPORT STRUCTURE	0.60	RETAINER STRAPS	0.35
INSULATION	0.90	SUPPORT STRUCTURE	0.90
	3.33	INSULATION	0.50
			3.12

Fig. 13 Leading edge weight breakdown.

edge concept, was that the heat pipes, by reducing the temperature, would permit the use of a lighter, less expensive structural material such as Hastelloy-X instead of columbium or carbon-carbon. However, the heat pipe design required a round cross section to efficiently contain the pressure of the working fluid. Round tubing is a less efficient cross section when used to carry bending moments than the trapezoidal cross section used in non-pressurized designs such as the columbium concept. The wick and working fluid, which are nonstructural, and the round cross section represent additional weight. This study indicates that the weight reduction possible by choice of material does not compensate for the weight penalties due to the wick, working fluid, and round cross section. In this configuration, the heat pipe concept is heavier than other candidates. The weights of the three uncooled concepts were not sufficiently different to permit a choice based on weight alone. It must be noted, however, that these results apply only to the Phase B design Shuttle orbiter.

General Considerations and Conclusions

In addition to weight and cost considerations, a number of less readily quantified but nonetheless important considerations affect the trade study outcome. These include material availability, fabricability, prior experience with the material, and material property characteristics. Some of these considerations are summarized in Fig. 14, along with weight and cost figures.

The heat pipe and ablator concepts use materials that are readily fabricated, as demonstrated by the design and construction of two heat pipe test segments reported in Ref. 3 and extensive experience with ablators. The heat pipe concepts would require inspection and verification of pipe operation. This would require ground operations, but would yield positive evidence of system integrity. Heat pipes might prove more susceptible to damage by meteoroid penetration than other concepts. The probability of catastrophic heat pipe leading edge damage was not computed but should be low because the design permits safe operation subsequent to the failure of nonadjacent heat pipes.

CONSIDERATION	HEAT PIPE HASTELLOY-X	ABLATIVE	CARBON-CARBON	COLUMBIUM
COST, MILLIONS OF DOLLARS TOTAL PROGRAM	36.94	107.96	33.29	32.82
WEIGHT - LB/FT^2	4.94	3.57	3.33	3.12
RELATIVE AVAILABILITY OF MATERIAL	1	1	2	1
RELATIVE FABRICABILITY	2	1	3	2
COMPATIBILITY (WORKING FLUID)	ACCEPTABLE	N.A.	N.A.	N.A.
RELATIVE FABRICATION EXPERIENCE	3	1	3	2
RELATIVE INSPECTIBILITY	2	1	2	3
OXIDATION (100 HR - 2000°F)	0.0003 IN	N.A.	COATING REQUIRED	COATING REQUIRED
PRIMARY DISADVANTAGE	WEIGHT	COST	FABRICATION EXPERIENCE AND FABRICABILITY	INSPECTION

N.A. - NOT APPLICABLE 1 - BEST 3 - WORST

Fig. 14 Leading edge trade study general considerations.

The ablative leading edge design was clearly the design candidate with the least uncertainty for successful development. Ablative materials used in previous programs are available; the structural materials selected are readily available, easily fabricated and have had wide prior application. The ablative leading edge would be somewhat susceptible to damage in installation and ground servicing. Subsequent to entry, the charred ablator would be rough in comparison with the other concepts and may be susceptible to rain erosion. Roughness would yield a higher wing drag. The ablative design probably would not suffer catastrophic damage due to meteoroid impact, because ablative materials offer good resistance to penetration and tend to heal under heating. Since the ablative TPS is replaced after each flight, no postflight inspection would be required. The new part would be inspected when manufactured. Because of very large refurbishment costs, the ablative version would be much more expensive than any of the other leading edge concepts.

The carbon-carbon concept utilized the material with the most uncertain development status. Carbon-carbon structures have been produced only in limited prototype quantities. Although feasible, they present the greatest TPS development risk of the candidate approaches. Inspection of carbon-carbon would be only slightly more difficult than an ablator, since the design could also provide for quick access. Replacement rate should be low and even though carbon-carbon was the most expensive material on a unit basis, the limited area requirement resulted in approximately the same cost as the other reusable designs. The carbon-carbon approach resulted in essentially the same weight as the columbium design and was lighter than either the ablative or heat pipe designs.

The columbium version resulted in estimated costs and weight approximately the same as the carbon-carbon. Columbium has been more widely used; consequently, fabrication experience and material availability are better than for carbon-carbon. This results in a lower development risk. The columbium leading edge would be difficult to inspect in place on the wing because columbium requires an oxidation protection coating. The coating would be subject to damage in ground handling and also to damage from meteoroid impact. The probability of coating damage from a meteoroid impact would be greater than the probability of penetration of a heat pipe in that TPS design. However, local coating damage should not result in a catastrophic failure.

In summary, reusable concepts all cost roughly the same and were found to be much less expensive than the nonreusable ablative TPS. The carbon-carbon and columbium designs weigh less than the heat pipe design. The choice between carbon-carbon and columbium is not obvious for the environment considered. Since the columbium version is simpler to fabricate and involves less development risk (because of the greater fabrication experience), it was considered the preferred concept for the Phase B orbiter.

References

[1] "Study of Structural Active Cooling and Heat Sink Systems for Space Shuttle, Final Report," Rept. E0638, June 30, 1972, McDonnell Douglas Corp., St. Louis, Mo.

[2] Mezines, S. A., "A Semi-Empirical Method for Correlating the Thermal Performance of Charring Ablative Materials," AIAA Paper 68-757, Los Angeles, Calif., 1968.

[3] "Design, Fabrication, Test and Delivery of Shuttle Heat Pipe Leading Edge Test Modules, Final Report," Rept. E0775, April 20, 1973, McDonnell Douglas Corp., St. Louis, Mo.